Cumulative Deformation Analysis of Foundation of Mined-Out Areas under Dynamic Loading - a Case Study of Taijiao High-Speed Railway

Kunpeng SHI, Shuren WANG*, Yubo CHEN, Wenfu YANG, Chunliu LI

Abstract: Since there is a safety risk of cumulative deformation exceeding the limit when high-speed rail passes through the mined-out areas, for the special needs of risk control along the high-speed railway, taking the foundation of the mined-out areas of Dianshang coal mine under Taijiao high-speed railway as the background, the mechanical model of rotation structure of key block was established. The stability criterion of fracture structure rock of the mined-out area was proposed. Using self-developed similar model test and dynamic loading device, the evolution characteristics and deformation mechanism of foundation of the mined-out areas under long-term dynamic loading of the high-speed railway were analyzed. Results show that when the number of loading vibration exceeds 5 million times, the foundation of the mined-out areas will occur over all settlement and deformation. The cumulative deformation of the foundation in different buried depths has similar variation law with the increasing of excitation and all experience three stages: the slow growth stage, the fast growth stage, and the stable stage. The prediction model of cumulative deformation of the foundation of the mined-out areas with different damage degrees under the long-term dynamic loading was proposed. The model parameters are closely related to the damage degree of foundation of the mined-out areas. The conclusions obtained in this study provide a theoretical basis for the prediction and control of the cumulative deformation of the foundation of the mined-out areas under the dynamic loading of high-speed railway.

Keywords: cumulative deformation; dynamic loading; foundation; high-speed railway; mined-out areas

1 INTRODUCTION

With the increasing of construction density of high-speed railway network in China, the available land resources are decreasing day by day, and some high-speed railway lines have to cross the mined-out areas. When high-speed railway passes the damaged foundation of the mined-out areas, the repeated vibration of the composite structure of the track subgrade and the foundation of the mined-out areas not only weaken its dynamic stability, but also cause excessive cumulative deformation, which may lead to the instability and damage of the subgrade structure in severe cases [1][2].

Under the action of cyclic dynamic loading of high-speed railway, the additional stress generated by the foundation of the mined-out areas may break the relative balance state of the damaged overburden stress in the mined-out areas, reactivate the mined-out areas, resulting in additional movement and cumulative deformation of the surface, which seriously affects the planning and construction of high-speed railway above the mined-out areas, and poses serious potential risks and safety hazards to the normal operation and maintenance of the high-speed railway [3]. The special geotechnical engineering conditions of the mine-out areas can make the problems of foundation settlement of the high-speed railway more prominent and more risky. Therefore, in view of the management and control needs of potential safety hazards along the high-speed railway, it is a challenging problem to be solved urgently for the construction and operation of the high-speed railway to study the cumulative deformation mechanism of the foundation in the mined-out areas under the dynamic loading of the high-speed railway [4, 5].

Under the action of long-term vibration loading, the stability analysis of the foundation deformation of the mined-out areas under the dynamic loading of the high-speed railway is of important theoretical meaning and engineering practical value to avoid the disaster of the high-speed railway.

2 STATE OF THE ART

To analyze the deformation control of the foundation of the mined-out areas under dynamic loading of the high-speed railway is still a relatively new topic, and the related results are in the stage of empirical exploration. Malnowska et al. proposed a method for predicting surface deformation of mining subsidence based on the influence function [6]. Strzalkowski et al. used the resistivity tomography to evaluate the possibility of surface collapse in selected areas of shallow mining [7]. Based on the probability integral model, Huang et al. conducted the dynamic analysis of the residual deformation in goaf [8]. Wang et al. analyzed the deformation response characteristics of the subgrade of the high-speed railway in the mined-out areas [8]. Shi et al. analyzed the surface deformation indexes with different mining sequences in multiple coal seams and revealed the sequence effects of mining time on the surface deformation in the goaf collapse areas [8]. Jiang and Wang established the prediction model of surface subsidence of the mined-out area under long-term train dynamic load by on-site monitoring and numerical simulation [9]. Gruszczynski et al. took the mined-out area of silesia coal mine in Poland as the background, and they conducted a comparative analysis of the parameters of different surface deformation models [8].

The stability of overburden roof in mined-out areas is the premise to ensure the safe use of superstructure. Srivastava et al. used self-potential and electrical resistivity tomography techniques to monitor the deformation of the abandoned roadways and surface in the old mining area under the railway, and they established a stability evaluation model for the abandoned mines [8]. Zhou et al. carried out indoor model test and numerical simulation to reveal the deformation characteristics of surrounding rock during tunnel excavation under the mined-out areas [14]. Yi et al. established an indoor test model to reveal the influence of long-term cyclic dynamic load of high-speed railway on the cumulative deformation of subway tunnel

lining [15]. Qin et al. proposed an improved algorithm suitable for evaluating goaf stability [16].

The safe operation of high-speed railway is not only related to regional stability and economic development, but is also related to the safe travel of hundreds of millions of people. Exploring the deformation characteristics of foundation under long-term vibration load of high-speed railway can provide theoretical basis and technical support for deformation control of the foundation of the mined-out areas. Wang et al. carried out the adaptability analysis of the coordinated deformation of the track structure of high-speed railway and subgrade, subgrade and the foundation of the mined-out area [8]. Gao et al. established the calculation method of cumulative deformation of subgrade and foundation under cyclic dynamic load of train [8]. Based on the critical state theory, Chen et al. proposed a simplified calculation method to describe the three-dimension cyclic cumulative deformation of soil, and they revealed the cumulative residual deformation of peat soil under long-term cyclic loading [8]. Wang et al. proposed a prediction model of the cyclic cumulative deformation of the subgrade under the train load. The applicability of the prediction model was verified by the full-scale subgrade model test [8]. However, the above mentioned deformation prediction models of high-speed railway foundation are not suitable for the prediction of the cumulative deformation of the foundation with damage.

Taking the foundation of Taijiao high-speed railway above the mined-out areas of Dianshang coal mine as the engineering background, the mechanical model of the overburden key block of the mined-out areas was established. The stability evaluation system of fractured strata of the mined-out areas was constructed. Then, through the indoor physical model test, the long-term dynamic loading of the high-speed railway was simulated, the structure evolution of the foundation and its deformation were analyzed, and the deformation prediction model of the foundation of the mined-out areas was proposed.

The remainder of this study is organized as follows. In Section 3, the engineering background is introduced, the stability analysis of the foundation of the mined-out areas is analyzed, the experiment model, the rainfall and dynamic loading conditions are stated. In Section 4, the experimental results are analyzed and discussed. Finally, some conclusions are given in Section 5.

3 METHODOLOGY
3.1 Engineering Background

The Taijiao high-speed railway passed the mined-out areas of Dianshang coal mine in Shanxi province, China, which was located about 2.3 km northeast of Gaoping city. The coal seam No. 3 was mainly mined, with a buried depth of 67.60 - 73.70 m and a thickness of 4.20 - 5.30 m, with an average thickness of 4.85 m. The ratio of mining depth to the thickness is 17.2 < 30, which is a typical shallow mined-out areas.

The residual deformation of the surface of the mined-out areas has a large range and a long time span, which causes irreversible damage and deformation to the surface and superstructure. As shown in Fig. 1, the residual deformation of foundation of the mined-out areas of Dianshang coal mine leads to the surface deformation and fruit trees dumping.

Figure 1 Residual deformation of the foundation of the mined-out areas

3.2 Theoretical Analysis

By using Image J processing software, the fracture mesh of the foundation in the mined-out areas under different rainfall was extracted as shown in Fig. 2. As seen from Fig. 2, after the initial separation of overburden strata in the mined-out areas, the fault blocks rotate under the action of upper load and dead weight, and the blocks squeeze and occlude each other, resulting in a hinged relationship under the action of horizontal thrust. At this point, the ends of the block are in the state of surface contact, and the friction between the contact surfaces, horizontal thrust and lower supporting force will directly affect the failure mode of the rock block [22-24]. Therefore, the stress distribution characteristics of the rock blocks are very important for the stability analysis of the foundation of the mined-out areas.
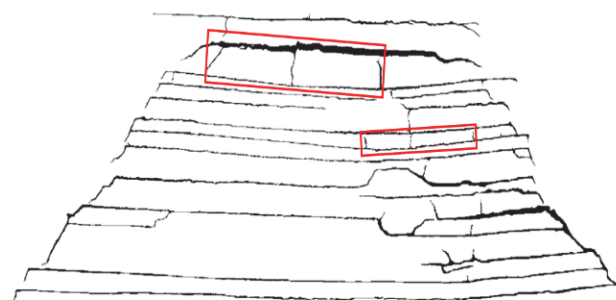

Figure 2 Fracture grid of the foundation

As shown in Fig. 3, the rotary mechanical model of fault overburden of the mined-out areas is established, and the horizontal stress distribution of rock block conforms to Eq. (1).

$$f(x) = \sigma_t (-h)^{-b} (x-h)^b \qquad (1)$$

where, $f(x)$ is the horizontal stress distribution function, σ_t is the horizontal stress, $0 \le b \le 2$, h is the distribution range of the horizontal stress.

According to the distribution law of horizontal stress of rock block and the contact geometry relationship after

rotation, the horizontal thrust T and its action position a can be obtained, respectively:

$$T = \sigma_t \int_0^h f(x) \mathrm{d}x \tag{2}$$

$$a = \frac{1}{2}(H - L\sin\alpha) \tag{3}$$

where, h is the height of rock block, L is the length of rock block, α is the inclination of the left rock block.
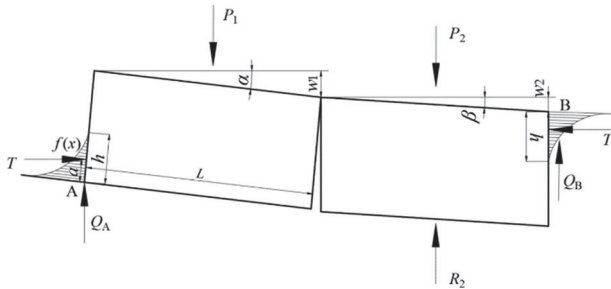

Figure 3 Mechanical model of fracture overburden

As seen from Fig. 3, the moment $\sum M_A = 0$ of the hinge point A and the vertical resultant force $\sum F_y = 0$ can be obtained:

$$T[H - 2a - L(\sin\alpha + \sin\beta)] = P_1(\frac{L}{2}\cos\alpha + H\sin\alpha) +$$
$$(P_2 - R_2)(L\cos\alpha + \frac{L}{2}\cos\beta + H\sin\beta) - \tag{4}$$
$$Q_B[L(\cos\alpha + \cos\beta - \sin\alpha - \sin\beta) + H]$$

$$\sigma_t \geq \frac{(P_1 + P_2)(b+1)\left[L(\frac{3}{4}\cos\alpha - \sin\alpha + \sqrt{2}\cos(45° + \beta) + H(1 - \frac{1}{2}\sin\alpha))\right]}{h\{0.3[\sqrt{2}L(\cos(45° + \alpha) + \cos(45° + \beta)) + H] + \sin\beta\}} \tag{9}$$

Then let $i = H/L$, i represents the ratio of the height of the rock layer to the length of the rock block, referred to as the fracture degree, then Eq. (10) can be obtained:

$$\sigma_t \geq \frac{(P_1 + P_2)(b+1)\left[(\frac{3}{4}\cos\alpha - \sin\alpha + \sqrt{2}\cos(45° + \beta) + i(1 - \frac{1}{2}\sin\alpha))\right]}{h\{0.3[\sqrt{2}(\cos(45° + \alpha) + \cos(45° + \beta)) + i] + \sin\beta\}} \tag{10}$$

As seen from Eq. (10), when the overlying load of the key block in the masonry beam is constant, that is, $P_1 + P_2$ is a constant, the conditions for the sliding instability of this structure are directly related to the fracture degree i and the rotation of the rock block in the masonry beam α and β.

3.3 Physical Model Experiment
3.3.1 The Prepared Experiment Model

Taking the foundation of Taijiao high-speed railway above the mined-out areas of Dianshang coal mine, China as the engineering background, the model test was carried out by using a combined multifunctional servo control

$$P_1 + P_2 = Q_A + Q_B + R_2 \tag{5}$$

where P_1 and P_2 are the loads borne by the rock blocks. R_2 is the support force of the rock block, α, β is the inclination of the rock block, respectively. Q_A, Q_B is the shear force of the rock block, respectively.

According to the calculation of the whole structure of the masonry beam, $R_2 = 1.03 P_2$, so it can be approximately regarded as $R_2 = P_2$, which can be obtained by substituting it into Eq. (4) and Eq. (5):

$$Q_B = \frac{\gamma L(H + H_1)(\frac{L}{2}\cos\alpha + H\sin\alpha) + T\sin\beta}{L(\sqrt{2}(\cos(45° + \alpha) + \cos(45° + \beta)) + H} \tag{6}$$

$$Q_A = \frac{(P_1 + P_2)\left[L(\frac{3}{4}\cos\alpha - \sin\alpha + \cos(45° + \beta) + H(1 - \frac{1}{2}\sin\alpha)) \right] - T\sin\beta}{L(\sqrt{2}(\cos(45° + \alpha) + \cos(45° + \beta)) + H} \tag{7}$$

The maximum shear force Q_A of this structure occurs at point A. In order to prevent the structure from slipping and becoming unstable at point A, the following condition must be met:

$$T\tan\varphi \geq Q_A \tag{8}$$

where, $\tan\varphi$ is the friction coefficient between masonry beam and rock blocks, generally taken as 0.3.

Substituting Eq. (8) into Eq. (7), Eq. (9) can be obtained:

loading test platform. The platform is 3500 cm long, 64 cm wide, and 2100 cm high. The non-linear loading system is distributed on both sides and the top of the platform, which is used to realize the horizontal and the upper loading. The loading range of the hydraulic servo system is 0.1 - 100 kN, which meets the experimental requirements.

According to the three theorems of similarity theory, the objective factors such as the size of similar model test-bed and the construction conditions of test site are comprehensively considered. The geometric similarity constant C_l of the experimental model was 0.01, the average density of the strata was 2400 kg/m³, and the dry density of the similar materials used in the test was

1600 kg/m³. The similarity constant of the density was $C_\rho = 1600/2400 = 0.67$. The similarity ratio of the physical quantities of the model was determined by the dimensional analysis method.

According to the similar ratio of similar materials, fine river sand, lime and gypsum were selected as the main raw materials for the test. The fine river sand below 0.5 mm was used as aggregate, lime and gypsum were used as main cementing materials, and the borax was added as the retarder. Since it is extremely difficult for the materials to strictly follow the similar ratio and fully meet the mechanical properties, the uniaxial compressive strength of the similar materials was selected as the main reference index in this test. Similar materials with different proportions were mixed and made into several 50 × 100 mm cylindrical standard samples. Taking the sample 337 with proportion number as an example, the pressure tester was used at a loading rate of 1 mm/min. After loading for 270 s, the specimen was destroyed with the peak stress of 0.58 MPa. In the similar model, each rock layer corresponds to the similar material ratio, as shown in Tab. 1.

Table 1 Similar materials proportion of the model

Lithology	Proportion number	Compressive strength / MPa	Actual density / kg/m³
Subgrade	537	18.80	1800
Loess	573	21.30	1980
Bedrock	537	22.60	2100
Mudstone	437	26.92	2250
Sandy mudstone	473	23.88	2300
Medium sandstone	455	25.16	2400
Siltstone	337	37.80	2600
Coal	573	20.00	1500

3.3.2 Test Platform and Dynamic Loading Conditions

The size of the test model is 275 cm long, 30 cm wide and 93 cm high, and the thickness of the coal seam is 4.05 m. After the model was laid and consolidated, the black random speckles were sprayed on the surface of the model with ink, and the coal seam was excavated after the monitoring equipment being installed, as shown in Fig. 4.
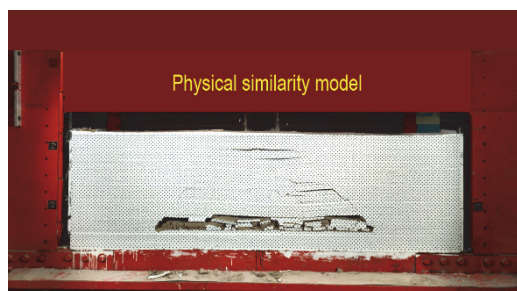

Figure 4 Speckle of physical similarity model

The three-dimension optical digital speckle strain measurement system (XTDIC) was adopted as the displacement monitoring equipment, which was composed of heavy camera support, a pair of high-precision industrial cameras, a camera controller, and a pair of LED fill lights, as shown in Fig. 5.

The XTDIC test and analysis system combined the digital image related technology and binocular stereo vision technology, the deformation trajectory of the seeds

was tracked by continuous shooting with high-precision cameras. Finally, the collected images were imported into the calculation module for analysis, which could realize the measurement of three-dimension coordinates, displacement, and strain on the surface of the measured object. In addition, the displacement accuracy of the test analysis system was in micron level, and the monitoring results could ensure the validity and accuracy of the prediction of the accumulated deformation of the foundation.

Figure 5 XTDIC test

The vibration exciter DH40500 was used as dynamic loading of the high-speed railway, and the sweep signal generator DH1301 was used as the control device of the vibration exciter, as shown in Fig. 6. The exciter would provide a variety of loading waveforms, which could meet the requirements of simulating the wheel-rail force generated during the high-speed railway running. In this test, the vibration load was applied to the foundation for more than 10 million times by loading device. According to the literature [25], the cyclic dynamic load of 4 million vibration times could be approximately equivalent to the load amount of train operation for 10 years.
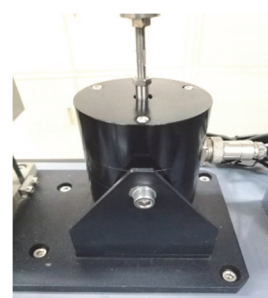

Figure 6 Dynamic loading device

4 RESULTS ANALYSIS AND DISCUSSION
4.1 Evolutionary Characteristics Analysis of Foundation

After the similar model was paved, compacted, consolidated and dried in layers, a simulated working face was established 55 cm away from the left boundary of the model. The working surface was mined 5 cm each time, for a total of 165 cm. After the coal seam being mined was stable, the model was pre-ballasted to accelerate the residual deformation of the foundation, and then simulated the deformation evolution of the foundation in the mined-out areas under the action of vibration load.

With the increase of vibration times of train dynamic load, the structural evolution and cumulative deformation of the foundation of the mined-out area are shown in

Fig. 7. As seen from Fig. 7a, in the initial stage of dynamic load loading, the foundation of the mined-out area had different degrees of small deformation in a large area. At this time, the deformation of the foundation of the mined-out area was mainly concentrated within 5 - 10 m from the surface and the step rotation in the lower right corner. With the continuous increase of dynamic load vibration, the main deformation position of the foundation was transferred to the zone of separation crack 10 - 15 m away from the surface. In addition, the deformation of the loose rock layer at the turn of the step also increased gradually, as shown in Fig. 7b.

When the number of dynamic load vibrations reached 7.5 million, the deformation range of the foundation of the mined-out area gradually spread to the surrounding and deep. At the same time, the strata separation and joints in the foundation of the mined-out area showed a closed trend, as shown in Fig. 7c. The number of dynamic load vibrations continued to increase, and the cumulative deformation of the foundation in the mined-out area gradually shifted to the rotary fracture of the rock block on the right. The rock stratum at the turning of the step was further compacted, and the inclination of the broken rock stratum increased accordingly. In addition, the width of the separation layer cracks in the upper part of the foundation decreased slowly and closed gradually, as shown in Fig. 7d.
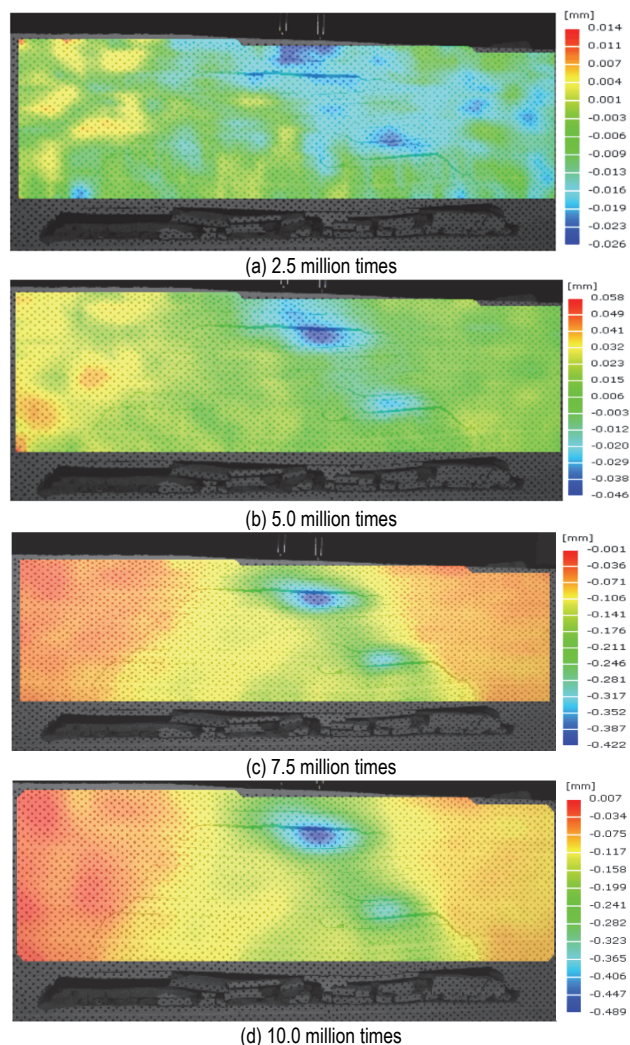

(a) 2.5 million times

(b) 5.0 million times

(c) 7.5 million times

(d) 10.0 million times
Figure 7 Deformation evolution characteristics of the foundation

As can be seen from Fig. 7, when the number of dynamic vibrations did not exceed 5 million, the cumulative deformation of the foundation in the mined-out areas was small and localized, and the deformation was mainly concentrated within 15 m from the surface depth. When the number of load vibrations exceeded 7.5 million, the foundation of the mined-out areas will have integral settlement deformation along the left and right fracture boundaries of the overburden.

4.2 Cumulative Deformation Analysis of the Foundation

The most intuitive and important damage of the long-term high-speed railway dynamic load to the foundation is cumulative settlement deformation. When the cumulative deformation of the foundation of the mined-out area exceeds the allowable settlement of high-speed railway foundation, it will seriously affect the safe operation and maintenance of high-speed railway. In this section, two vertical monitoring lines of cumulative deformation of foundation were arranged directly below the dynamic loading device, as shown in Fig. 8. The monitoring data collected by the three-dimension optical speckle system were extracted to obtain the cumulative deformation of the foundation of the mined-out areas under the long-term train dynamic load, as shown in Fig. 9.
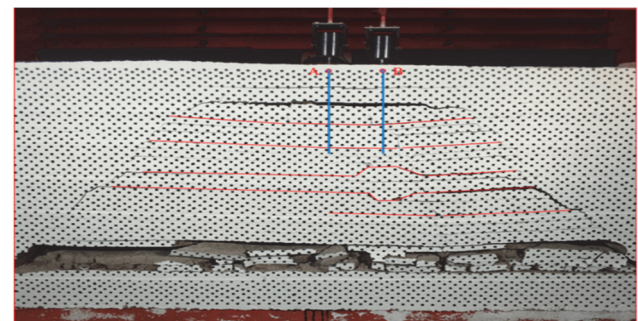

Figure 8 Monitoring line of the accumulation deformation of the foundation

As seen from Fig. 9, under the action of cyclic dynamic load of train, the cumulative deformation variations of the foundation of the mined-out areas with vibration times are similar, and they all go through three stages: the slow growth stage, the fast growth stage, and the stable stage. In the initial stage of train dynamic loading, the cumulative deformation of the foundation of the mined-out area was relatively stable, and the vibration amplitude of the displacement always fluctuated within 0.02 mm, without deformation accumulation. With the increase of the number of load vibrations, the deformation of the foundation increased slowly. The overall sudden deformation of the foundation appeared, which was basically consistent with the deformation characteristics of the foundation in previous section. Finally, the deformation tended to be stable after the dynamic load vibration of the train exceeding 8 million times.

It can be seen from Fig. 9, before the overall sudden subsidence of the foundation, the left-line monitoring points with a buried depth of more than 16 m had an upward arch phenomenon. However, in the same loading stage, in some monitoring points on the right line occurred settlement deformation. When the overburden of the mined-out area was unstable and damaged, the middle part

sunk at the fracture of the rock stratum, the step rotation, and the two ends were upturned, which was consistent with the variation characteristics of the inclination of the overlying rock of the mined-out areas in Fig. 10. Due to the fact that the simply supported beam structure above the interlayer cracks did not break, the deformation of the surface was relatively mild, and the sudden change was not obvious.
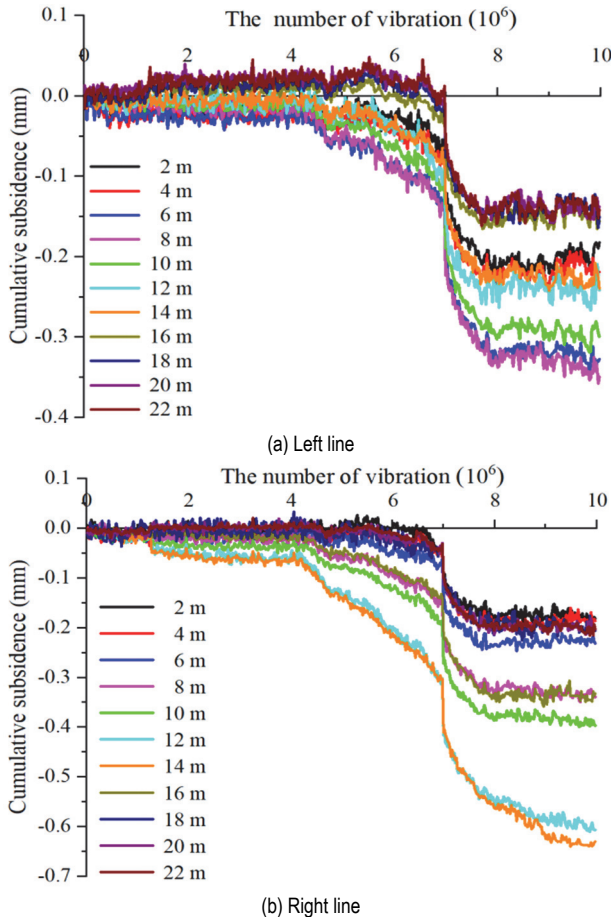

Figure 9 Variation of the accumulated deformation of foundation with the vibration number of load
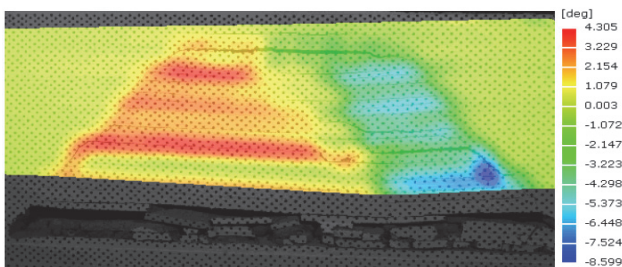

Figure 10 Variation characteristics of the inclination of the overburden

4.3 Deformation Analysis of Foundation along the Depth

Under the action of long-term vibration load, the accumulated deformation of the strata at different depths in the foundation of the mined-out areas reflects the stability and compactness of corresponding positions. It is of great engineering significance to explore the cumulative deformation of the foundation of the mined-out area at different depths for the prediction and control of cumulative deformation. Therefore, it is necessary to study the deformation law of the foundation along the depth. The

deformation characteristics of the foundation along the depth are shown in Fig. 11.

As seen from Fig. 11, with the increase of the buried depth, the cumulative deformation of the foundation of the mined-out area firstly increased and then decreased. Due to the influence of the depth of the train load and the different damage degrees at different positions of the foundation, from the comparison of Fig. 11a and Fig. 11b, the maximum cumulative deformation on the right was located at the buried depth of about 13 m, while the left side was about 8 m, and the deformation of the former was nearly twice that of the latter. In addition, from the deformation at both ends of the curve, the overall deformation of the foundation of the mined-out areas was in the range of 0.1 - 0.2 mm. Overall, under the long-term vibration load of the train, the most unstable and deformation prone area in the foundation of the mined-out areas was not the surface and near-field overburden of the mined-out areas, but the interlayer separation area where the rock stratum broke. In addition, the two deformation curves of the foundation in Fig. 11 showed approximately symmetrical distribution along the cumulative deformation peak, and the deformation approximately met the Gaussian function relationship, the correlation coefficients of the fitting curves are all above 93%:

$$y = m + ne^{-2\frac{(x-w)^2}{r}} \tag{11}$$

where, y is the cumulative deformation, x is the depth, and m, n, w and r is the constant, respectively.
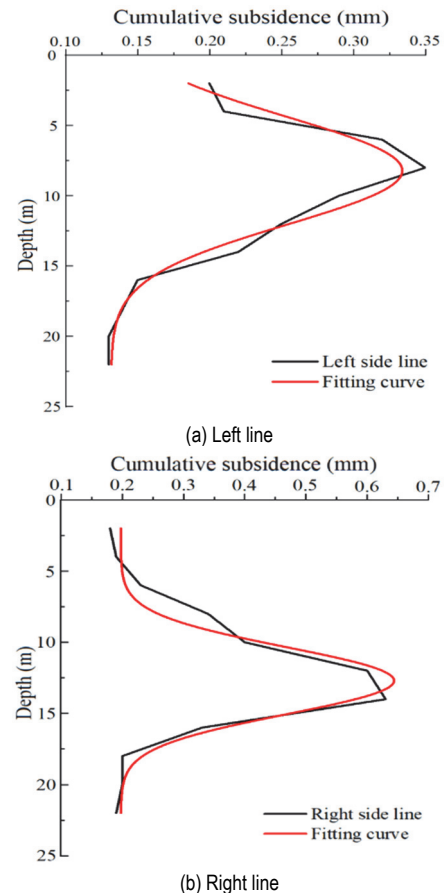

Figure 11 Deformation law of the foundation along the depth

4.4 Prediction Model of Cumulative Deformation of the Foundation

Many cumulative deformation models were established to predict the cumulative deformation of soil under cyclic loads through the indoor and outdoor experiments, theoretical analysis and numerical simulation. The most widely used and earliest empirical model of soil cumulative deformation is the Monismith index model [26]:

$$\varepsilon_p = aN^b \tag{12}$$

where, ε_p is the cumulative plastic strain, N is the loading times, a, b are constants.

In Monismith prediction model, the physical meaning of parameter a is not clear, and the model has great discreteness for different types and stress states of the soil. Li and Selige found that parameter a in Monismith model was closely related to dynamic deviator stress ε_d and static strength of soil ε_f through dynamic triaxial test results of soil [27]. Therefore, on the basis of Monismith model, the following expression is proposed:

$$\varepsilon_p = a\left(\frac{\sigma_d}{\sigma_f}\right)^m N^b \tag{13}$$

where, a, m and b are the material parameters.

Based on the test results of Samang, Chai et al. proposed the following expression [28]:

$$\varepsilon_p = a\left(\frac{\sigma_d}{\sigma_f}\right)^m \left(1 + \frac{\sigma_s}{\sigma_f}\right)^n N^b \tag{14}$$

where, ε_s is the initial static deviator stress, a, b, m reflect the stress state, the physical state and the type of soil.

The above-mentioned prediction model of the cumulative deformation of the soil under cyclic loading was obtained by the dynamic triaxial tests of non-damaged remodelled soil samples, which is not suitable for the prediction of cumulative deformation of the damaged foundation of the mined-out areas. Taking two points A and B on the surface as examples, the variation curves of cumulative deformation of the foundation under the vibration load collected by three-dimension optical speckle system are shown in Fig. 12.
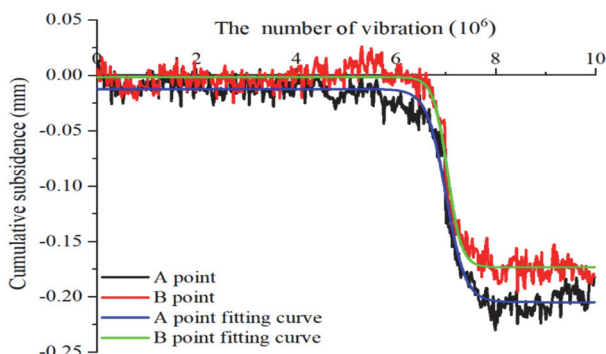

Figure 12 Relationship between the settlement of the surface and load vibration times

The fitting curve meets the variation characteristics of Boltzmann function, and its fitting correlation coefficients are more than 98%:

$$y = a + \frac{b}{1 + e^{(N-c)/d}} \tag{15}$$

where, N is the number of dynamic load vibration, a, b, c and d reflect the stress condition, physical state, soil type of the rock strata, respectively.

It can be seen from Fig. 12, the cumulative deformation of the foundation of the mined-out areas increased slowly with the number of the vibration load, then increased sharply, and finally the deformation rate slowed down and gradually tended to be stable. This is different from the fact that the cumulative deformation rate of undamaged soil was large in the early stage, gradually slowed down in the middle stage and finally tended to be stable. Under the long-term dynamic load of trains, the damage degree of the foundation of the mined-out areas with different buried depths is different, and its cumulative deformation law is also different. According to the Boltzmann function, the cumulative deformation of the foundation of the mined-out areas at different depths was fitted, and the variation curves of the fitting parameters with the buried depth are shown in Fig. 13.
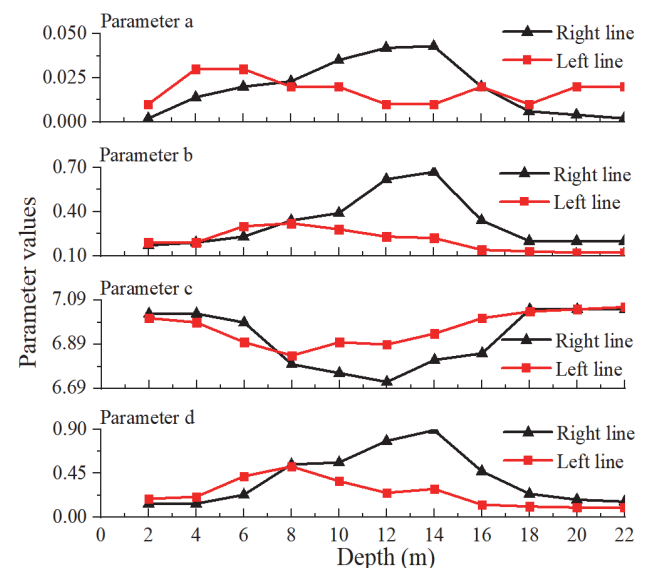

Figure 13 Variation of the fitting parameters with the buried depth of the foundation

As seen from Fig. 13, the fluctuation degree of parameter a with the depth was small, which mainly controls the initial value of the cumulative deformation of the foundation of the mined-out areas. In addition, according to the comprehensive analysis of Fig. 13, the value range of parameters b, c and d is 0.1 - 0.7, 6.6 - 7.2 and 0 - 1, respectively, and these values are related to the damage degree of the foundation. Under the long-term action of the vibration load, the more prone to deformation failure in the foundation of the mined-out areas, the greater the value of parameters b and d in the prediction model of the cumulative deformation, and the smaller the value of parameter c.

5 CONCLUSION

Taking the foundation of the mined-out areas in Dianshang coal mine as the engineering background, analytical methods, physical tests and numerical simulations were used to reveal the cumulative deformation characteristics of the foundation of the mined-out areas under the high-speed railway. The main conclusions are obtained as the following:

(1) The mechanical model of the fractured rock strata of the foundation of the mined-out areas is established, the instability criterion of the key block of the masonry beam in the mined-out areas is obtained. At the initial stage of train vibration load, the local deformation occurs only at the relatively unstable position of the foundation. After the vibration times of dynamic load exceeding 5 million times, the foundation of the mined-out area will have overall settlement.

(2) Under the action of train vibration load, the variation characteristics of cumulative deformation of the foundation of the mined-out area with vibration times is similar, which has experienced three stages: the slow growth stage, the fast growth stage, and the stable stage. The cumulative deformation mainly occurs in the first 8 million vibration stages, accounting for about 91% of the total cumulative deformation.

(3) The long-term dynamic load of high-speed railway has a great impact on the fracture and separation of foundation strata and the rotation of steps in the foundation. The cumulative deformation prediction model of the foundation of the mined-out area with different damage degrees under long-term train load is proposed. The value of model parameters is closely related to the damage degree of the foundation.

This study can provide the reference for the prediction and control of the cumulative deformation of the foundation of the mined-out areas. However, the long-term dynamic stability of the foundation in the mined-out areas under the heavy-haul railway and the anchor-grouting reinforcement of the foundation needs to be paid attention [29-31], the deformation mechanism, dynamic response, and the reinforcement counmeasures of the foundation of the foundation will be further studied under the long-term load of trains with different axle loads and running speeds.

Acknowledgements

6 REFERENCES

[1] Helm, P. R., Davie, C. T., & Glendinning, S. (2013). Numerical modelling of shallow abandoned mine working subsidence affecting transport infrastructure. *Engineering Geology*, *154*, 6-19. https://doi.org/10.1016/j.enggeo.2012.12.003

[2] Luo, Z. Q., Xie, C. Y., Zhou, J. M., & Jia, N. (2015). Numerical analysis of stability for mined-out area in multi-field coupling. *Journal of Central South University*, *22*(2), 669-675. https://doi.org/10.1007/s11771-015-2569-8

[3] Ntotsios, E. (2021). Ground vibrations from high-speed railways: prediction and mitigation. *Journal of Sound and Vibration*, *490*. https://doi.org/10.1016/j.jsv.2020.115563

[4] Gao, Y., Huang, H., Ho, C. L., & Hyslip, J. P. (2017). High speed railway track dynamic behavior near critical speed. *Soil Dynamics and Earthquake Engineering*, *101*, 285-294. https://doi.org/10.1016/j.soildyn.2017.08.001

[5] Connolly, D. P., Dong, K. T., Costa, P. A., Soares, P., & Woodward, P. K. (2020). High speed railway ground dynamics: a multi-model analysis. *International Journal of Rail Transportation*, *8*(4), 324-346. https://doi.org/10.1080/23248378.2020.1712267

[6] Malinowska, A., Hejmanowski, R., & Dai, H. Y. (2020). Ground movements modeling applying adjusted influence function. *International Journal of Mining Science and Technology*, *30*, 243-249. https://doi.org/10.1016/j.ijmst.2020.01.007

[7] Strzalkowski, P., Scigala, R., Szafulera, K., & Kolodziej, K. (2021). Surface deformations resulting from abandoned mining excavations. *Energies*, *14*(9), 2495. https://doi.org/10.3390/en14092495

[8] Huang, C. F., Li, Q., & Tian, S. G. (2020). Research on prediction of residual deformation in goaf of steeply inclined extra-thick coal seam. *Plos One*, *15*(10). https://doi.org/10.1371/journal.pone.0240428

[9] Wang, S. R., Shi, K. P., Zou, Y. F, Zou, Z. S., & Wojciechowski, A. (2021). Coupling deformation between non-uniform settlement of track-structure and subgrade of high-speed railway above the mind-out areas. *Acta Montanistica Slovaca*, *26*(4), 620-633. https://doi.org/10.46544/AMS.v26i4.03

[10] Shi, Z. Y., Wang, Q. B., Wang, P., He, D. L., & You, H. Y. (2020). Time series effect on surface deformation above goafarea with multiple-seam mining. *Symmetry*, *12*(9), 1428. https://doi.org/10.3390/sym12091428

[11] Jiang, S. & Wang, Y. M. (2019). Long-term ground settlements over mined-out region induced by railway construction and operation. *Sustainability*, *11*(3), 875. https://doi.org/10.3390/su11030875

[12] Gruszczynski, W., Niedojadlo, Z., & Mrochen, D. A. (2019). Comparison of methods for propagating surface deformation uncertainties in model parameters. Acta *Geodynamica et Geomaterialia*, *16*(4), 349-357. https://doi.org/10.13168/AGG.2019.0029

[13] Srivastava, S., Pal, S. K., & Kumar, R. (2020). A time-lapse study using self-potential and electrical resistivity tomography methods for mapping of old mine working across railway-tracks in a part of Raniganj coalfield, India. *Environmental Earth Sciences*, *79*(13). https://doi.org/10.1007/s12665-020-09067-3

[14] Zhou, Y., Feng, S. W., & Li, J. W. (2021). Study on the failure mechanism of rock mass around a mined-out area above a highway tunnel-Similarity model test and numerical analysis. *Tunnelling and Underground Space Technology*, *118*. https://doi.org/10.1016/j.tust.2021.104182

[15] Yi, H. Y., Qi, T. Y., & Qian, W. P. (2019). Influence of long-term dynamic load induced by high-speed trains on the accumulative deformation of shallow buried tunnel linings. *Tunnelling and Underground Space Technology*, *84*, 166-176. https://doi.org/10.1016/j.tust.2018.11.005

[16] Qin, Y. G., Luo, Z. Q., Wang, J., Ma, S. W., & Feng, C. D. (2019). Evaluation of goafstability based on transfer learning theory of artificial intelligence. *IEEE Access*, *7*, 96912-96925. https://doi.org/10.1109/ACCESS.2019.2929533

[17] Wang, S. R., Shi, K. P., Zhou, T. H., Zou, Y. F., & Hu, J. C. (2021). Foundation adaptability and subgrade deformation analysis of high-speed railway above the mined-out areas. *Journal of Engineering Science and Technology Review*, *14*(1), 170-177. https://doi.org/10.25103/jestr.141.20

[18] Wang, S. R., Shi, K. P., Zou, Y. F., Zou, Z. S., Wang, X. C., & Li, C. L. (2021). Size effect analysis of scale test model

for high-speed railway foundation under dynamic loading condition. *Technical Gazette*, *28*(5), 1615-1625. https://doi.org/10.17559/TV-20210208101312

[19] Gao, Z. L., Luo, X., Cai, D. G., Bian, X. C., & Chen, Y. M. (2022). Cyclic settlement of ballast layer due to train passages at high speed and its reduction by asphalt trackbed. *Construction and Building Materials*, *318*. https://doi.org/10.1016/j.conbuildmat.2021.125956

[20] Chen, C., Xu, G. F., Zhou, Z. M., & Kong, L. W. (2020). Undrained dynamic behaviour of peaty organic soil under long-term cyclic loading, part II: Constitutive model and simulation. *Soil Dynamics and Earthquake Engineering*, *129*. https://doi.org/10.1016/j.soildyn.2018.01.012

[21] Wang, H. L., Cui, Y. J., Ye, X. W., Lamas-Lopez, F., Dupla, J. C., Canou, J., Calon, N., Saussine, G., Aimedieu, P., & Chen, R. P. (2018). Permanent deformation of track-bed materials at various inclusion contents under large number of loading cycles. *Journal of Geotechnical and Geoenvironmental Engineering*, *144*(8). https://doi.org/10.1061/(ASCE)GT.1943-5606.0001911

[22] Li, Z. L., Dou, L. M., Cai, W., & Wang, G. F. (2016). Mechanical analysis of static stress within fault-pillars based on a voussoirbeam structure. *Rock Mechanics and Rock Engineering*, *49*(3), 1097-1105. https://doi.org/10.1007/s00603-015-0754-6

[23] Zhao Y. H., Wang, S. R., Zou, Z. S., Ge, L. L., & Cui, F. (2018). Instability characteristics of the cracked roof rock beam under shallow mining conditions. *International Journal of Mining Science and Technology*, *28*(3), 437-444. https://doi.org/10.1016/j.ijmst.2018.03.005

[24] Wang, S. R., Wu, X. G., Zhao, Y. H., Hagan, P., & Cao, C. (2019). Evolution characteristics of composite pressure-arch in thin bedrock of overlying strata during shallow coal mining. *International Journal of Applied Mechanics*, *11*(5). https://doi.org/10.1142/S1758825119500303

[25] Cai, Y., Xu, L. R., Liu, W. Z., & Shang, Y. H. (2019). Field test study on the dynamic response of the cement-improved expansive soil subgrade of a heavy-haul railway. *Soil Dynamics and Earthquake Engineering*, *128*, 105878. https://doi.org/10.1016/j.soildyn.2019.105878

[26] Monismith, C. L., Ogawa, N., & Freeme, C. R. (1975). Permanent deformation characteristics of subsoil due to repeated loading. *Transportation Research Record*, *537*, 1-17.

[27] Li, D. & Selig, E. T. (1996). Cumulative plastic deformation for fine-grained subgrade soils. *Journal of Geotechnical Engineering*, *122*(12), 1006-1013. https://doi.org/10.1061/(ASCE)0733-9410(1996)122:12(1006)

[28] Chai, J. C. & Miura, N. (2002). Traffic load induced permanent deformation of road on soft subsoil. *Journal of Geotechnical and Geo-environmental Engineering*, *128*(11), 907-916. https://doi.org/10.1061/(ASCE)1090-0241(2002)128:11(907)

[29] Li, D. Q., Ming, C., & Masoumi, H. (2021). A constitutive model for cable bolts exhibiting cone shaped failure mode. *International Journal of Rock Mechanics and Mining Science*, *145*, 104855. https://doi.org/10.1016/j.ijrmms.2021.104855

[30] Chen, J. H., Liu, P., Liu, L., Zeng, B. Q., Zhao, H. B., Zhang, C., Zhang, J. W., & Li, D. Q. (2022). Anchorage performance of a modified cable anchor subjected to different joint opening conditions. *Construction and Building Materials*, *336*. https://doi.org/10.1016/j.conbuildmat.2022.127558

[31] Li, D. Q., Li, Y. C., Chen, J. H. & Masoumi, H. (2021). An analytical model for the load-displacement behaviour of rock bolts based on continuously yielding criterion. *Tunnelling and Underground Space Technology*, *113*. https://doi.org/10.1016/j.tust.2021.103955

Contact information:

Kunpeng SHI, PhD, Candidate
School of Civil Engineering, Henan Polytechnic University,
No. 2001 Century Avenue, Jiaozuo, Henan Province, 454003, China
E-mail: 444583054@qq.com

Shuren WANG, PhD, Professor
(Corresponding author)
1) International Joint Research Laboratory of Henan Province for Underground Space Development and Disaster Prevention, Henan Polytechnic University, China
2) School of Minerals and Energy Resources Engineering, University of New South Wales, Sydney, NSW 2052, Australia
3) State Collaborative Innovation Center   Coal Work Safety and Clean-efficiency Utilization, Henan Polytechnic University, China
No. 2001 Century Avenue, Jiaozuo, Henan Province, 454003, China
E-mail: w_sr88@163.com

Yubo CHEN, PhD, Candidate
School of Civil Engineering, Henan Polytechnic University,
No. 2001 Century Avenue, Jiaozuo, Henan Province, 454003, China
E-mail: 569079218@qq.com

Wenfu YANG, PhD, Professor
Shanxi Provincial Key Lab of Resources, Environment and Disaster Monitoring, Coal Geological Geophysical Exploration Surveying & Mapping Institute of Shanxi Province,
No. 380 Yingbin West Street, Jinzhong, Shanxi Province, 030600, China
E-mail: wcyywf@163.com

Chunliu LI, PhD, Associate Professor
School of Urban Construction, Hebei Normal University of Science and Technology,
No. 360 Hebei West Street, Qingdao, Hebei Province, 066004, China
E-mail: lclcc_010@163.com